Original Article

Decellularized Sheep Peripheral Nerve: A Viable Alternative to Swine Xenografts for Peripheral Nerve Repair

Fajar Shodiq Permata[1*], **Muhammad Mirandy Pratama Sirat**[2, 3], **Rini Dharmastiti**[4, 5], **Rina Susilowati**[5, 6]

1. Laboratory of Veterinary Anatomy, Histology, and Embryology, Faculty of Veterinary Medicine, Universitas Brawijaya, Malang, Indonesia.
2. Department of Animal Husbandry, Faculty of Agriculture, Universitas Lampung, Bandar Lampung, Indonesia.
3 Doctoral Program of Veterinary Science, Faculty of Veterinary Medicine, Universitas Gadjah Mada, Yogyakarta, Indonesia.
4. Department Mechanical and Industrial Engineering, Faculty of Engineering, Universitas Gadjah Mada, Yogyakarta, Indonesia.
5. Biomedical Engineering Program, Graduate School of Universitas Gadjah Mada, Yogyakarta, Indonesia.
6. Department of Histology and Cell Biology, Faculty of Medicine, Public Health and Nursing, Universitas Gadjah Mada, Yogyakarta, Indonesia.

Use your device to scan and read the article online

How to Cite This Article Permata, F.S., Sirat, M. M. P., Dharmastiti, R., & Susilowati, R. (2026). Decellularized Sheep Peripheral Nerve: A Viable Alternative to Swine Xenografts for Peripheral Nerve Repair. *Iranian Journal of Veterinary Medicine, 20*(5), 975-986. http://dx.doi.org/10.22034/ijvm.20.5.1005877

http://dx.doi.org/10.22034/ijvm.20.5.1005877

ABSTRACT

Background: The widespread use of swine-derived biomaterials presents significant challenges in healthcare, particularly in regions with religious and cultural restrictions on the use of porcine products. This limitation necessitates the development of alternative xenograft sources for tissue engineering applications, such as those used in peripheral nerve repair. For tissue implants to be effective, they must closely mimic the biomechanical and structural characteristics of native tissue. While acellular xenografts from sheep are promising alternatives to swine-derived tissues, their application in peripheral nerve regeneration is limited by a lack of comprehensive characterization.

Objectives: This study aimed to comprehensively characterize fresh and decellularized peripheral nerve tissues from both sheep and swine.

Methods: Fourteen sciatic nerves from each species were divided into two groups: fresh and decellularized. Decellularization protocols, optimized for each species, involved a freeze-thaw cycle followed by immersion in 0.1% SDS-EDTA (14 days for sheep, 25 days for swine). Characterization included macroscopic evaluation, microstructural analysis, and mechanical testing.

Results: Decellularized sheep nerves had a significantly smaller diameter, fewer residual cellular components, and higher ultimate tensile stress ($P<0.05$) than decellularized swine nerves. Microstructural analysis revealed that endoneurial pore diameters ranged primarily from 3 to 12 µm, with a notable proportion exceeding 12 µm, suggesting the potential to integrate growth factors and cells to treat human peripheral nerve injuries (PNIs).

Conclusion: The superior decellularization efficiency, reduced residual cellular components, and enhanced mechanical properties observed in sheep nerves indicate their significant promise as a viable and effective substitute for swine-derived decellularized peripheral nerve grafts.

Keywords: Acellular tissue, Decellularization, Peripheral nerve, Tissue engineering, Xenograft

Article info:
Received: 18 Feb 2026
Accepted: 15 Apr 2026
Publish: 01 Sep 2026

*** Corresponding Author:**
Fajar Shodiq Permata, Assistant Professor.
Address: *Laboratory of Veterinary Anatomy, Histology, and Embryology, Faculty of Veterinary Medicine, Universitas Brawijaya, Malang, Indonesia.*
Phone: *+62 (85) 878214102*
E-mail: *drh.fajar@ub.ac.id*

Copyright © 2026 The Author(s);
This is an open access article distributed under the terms of the Creative Commons Attribution License (CC-By-NC: https://creativecommons.org/licenses/by-nc/4.0/legalcode.en), which permits use, distribution, and reproduction in any medium, provided the original work is properly cited and is not used for commercial purposes.

Introduction

Peripheral nerve injuries (PNIs) are a prevalent medical concern, frequently leading to significant sensory and motor dysfunction. These injuries, often resulting from trauma or surgical procedures, disrupt nerve pathway continuity, impairing signal transmission to target tissues, leading to Wallerian degeneration (Yu et al., 2016; Hussain et al., 2020). This degeneration creates an environment conducive to axonal regrowth, though complete functional recovery is often elusive (Deumens et al., 2010). Current therapeutic approaches to bridge nerve gaps include nerve conduits and grafts, which facilitate both axonal regeneration. While autologous nerve grafts remain the gold standard due to their optimal biocompatibility and growth-promoting cues, their use is limited by donor site morbidity and tissue availability. Consequently, nerve conduits are often constructed from various biomaterials, including acellular xenografts. These conduits provide a favorable microenvironment that actively promotes Schwann cell migration and axonal growth (Stang et al., 2009; Gu et al., 2011), offering advantages, such as reduced donor-site morbidity and the ability to bridge significant nerve gaps (Wang et al., 2015; Wolfe et al., 2023).

Despite these advancements, a significant challenge persists in finding suitable xenograft alternatives that minimize immunogenicity and maximize compatibility for nerve repair (Cooper et al., 2023). Swine-derived acellular grafts have been widely utilized in tissue engineering due to their abundance, anatomical similarities to human tissue (Azab & Youssef, 2021; Gabriel et al., 2024), and capacity to support tissue regeneration (Zhang et al., 2010; Zajicek et al., 2011). However, cultural and religious restrictions in certain regions prohibit the use of swine-derived products, necessitating the search for alternative xenograft sources. Early studies on acellular sheep tissues, including vascular and nerve tissues, demonstrate that decellularization can preserve essential extracellular matrix (ECM) components. This preservation is crucial for supporting nerve regeneration and providing a scaffold for Schwann cell migration and axonal growth (Contreras et al., 2022; Li et al., 2023).

The decellularization process is particularly advantageous as it significantly reduces immunogenicity, enhancing xenograft compatibility with host tissue. By removing cellular components while preserving the ECM, this process creates a biocompatible scaffold that can facilitate tissue repair without complications from immune rejection (Crapo et al., 2011). Acellular sheep nerve grafts have demonstrated efficacy in bridging nerve gaps and promoting axonal regeneration in preclinical models (e.g. Zhang et al., 2010), suggesting their potential clinical utility.

While sheep-derived xenografts offer a viable alternative, several critical gaps in the literature hinder a complete understanding of their potential in peripheral nerve repair. First, despite the well-documented anatomical, histological, and physiological similarities between sheep and swine and humans (Siemens et al., 1990; Firdaus et al., 2024; Sharmadha & Balakrishnan, 2024), there is limited research directly comparing the mechanical properties and structural integrity of peripheral nerves derived from these species. Most existing studies have focused primarily on swine-derived grafts, with comparatively fewer on sheep-derived grafts. A direct comparison of fresh and decellularized sheep and swine peripheral nerves is therefore necessary to validate sheep as a suitable alternative.

Second, much of the research on acellular nerve grafts has used small-animal models. However, more research involving larger animal models, such as sheep and swine, is crucial to better understand graft performance under conditions more closely resembling human peripheral anatomy and biomechanics (Sondell et al., 1998; Borschel et al., 2003; Yang et al., 2011; Tuffaha et al., 2020). A comprehensive examination of how decellularized ovine xenografts match the anatomical and mechanical properties required for effective nerve repair is essential for establishing their clinical applicability.

This study aimed to evaluate the potential of decellularized sheep peripheral nerves as a viable alternative to swine-derived xenografts for peripheral nerve repair. The novelty of this study lies in providing a detailed characterization of sheep-derived grafts against established benchmarks for swine grafts and human nerve properties. This research directly addresses a critical gap in the literature on alternative xenograft sources. This work makes a significant contribution to developing acceptable, biologically effective products, which expand treatment options for clinicians and patients in regions with specific religious or cultural restrictions on the use of swine-derived products.

Materials and Methods

Research samples

We collected 10 cm segments of sciatic nerves from female, 7-month-old sheep and swine. The sheep samples came from a private slaughterhouse in Kasihan, Bantul, Yogyakarta, Indonesia, while the swine samples were obtained from a private slaughterhouse in Godean, Yogyakarta, Indonesia. In total, we collected 14 sciatic nerves from each species. These were then divided into two groups: fresh nerves, taken from the right hindlimb, and decellularized nerves, obtained from the left hindlimb. The tissue collection procedure received approval from the Medical Ethics Committee of the Faculty of Medicine, Universitas Brawijaya.

Decellularization method

Upon collection, nerves were transported to the laboratory in a solution of 1% (w/v) penicillin-streptomycin (Wonder, USA) in normal saline (Otsuka, Japan) at pH 7.0. For overnight storage, the nerves were kept at -20 ˚C in a freezer (SHARP, Japan) with 20 mL of phosphate-buffered saline (PBS, pH 7.4) prepared according to a standard recipe (Green & Sambrook, 2012).

The following day, we immersed the nerves in 200 mL of decellularization solution within a 10 cm Petri dish (Iwaki, Japan) at room temperature. The solution consisted of 0.1% (w/v) sodium dodecyl sulfate (SDS, Merck, Germany) and ethylenediaminetetraacetic acid (EDTA, Sigma, USA). Sheep nerves were submerged for 14 days, while swine nerves required 25 days of immersion. The decellularization solution was refreshed every 3 days for both groups. After decellularization, the nerves were rinsed three times with PBS for 5 minutes each. This methodology was adapted and modified from previous studies (Zhang et al., 2010; Permata et al., 2012). SDS is a good detergent for decellularization of soft tissue (Permata et al., 2025). The difference in decellularization duration between sheep and swine was based on our preliminary optimization results. Swine sciatic nerves had a thicker epineurium and more abundant interfascicular adipose tissue, which hindered detergent diffusion and led to incomplete cell removal at shorter immersion times. Extending the immersion to 25 days resulted in better decellularization, with good ECM integrity and endoneurial pores (unpublished data). In contrast, sheep nerves—with less adipose content and thinner connective layers—achieved full decellularization within 14 days.

Macroscopic characterization

All fresh and decellularized nerves from sheep and swine were digitally photographed using a Canon CyberShot pocket camera (Japan). To measure nerve dimensions, we used a Vernier caliper (Taffware, China) to determine the long and short axes (denoted as ‘a’ and ‘b’ in millimeters). The mean diameter (d) was calculated using the geometric mean formula (Equation 1):

1. $d=\sqrt{ab}$ (Jahnke & Bedi, 2007).

Subsequently, we calculated the cross-sectional area of the nerves, assuming an oval shape, using the Equation 2 for the area of an ellipse.

2. $\text{Area } (mm^2)= \prod \times \frac{a}{2} \times \frac{b}{2}$

Microstructure characterization

For histological analysis, the 3 cm proximal nerve segments were first rinsed in PBS, then fixed in 4% formaldehyde for 24 hours. The next day, nerve segments underwent gradual dehydration through an ethanol series (Merck, Germany) from 70% to 100%, followed by clearing in xylene (JT Baker, Germany), and then infiltration and embedding in paraffin. Nerve paraffin blocks were serially sectioned at 10 µm thickness with a 1,000 µm spacing to yield 12 sections per sample. Finally, the nerve tissue sections were stained with hematoxylin and eosin (H&E).

To ensure unbiased sample selection at higher magnification, five representative areas from the low-magnified image—the upper-left corner, upper-right corner, middle, bottom-left corner, and bottom-right corner—were randomly selected and photographed at high magnification. For the decellularized group only, we quantified the remnants of nerve fiber components and measured the diameter of endoneurial pores directly from images of nerve fascicles. The area of the 2D nerve section was about 11-16 mm^2, depending on nerve size, and each representative area with higher magnification (100x magnification) was 1 mm^2; thus, the total representative area was about 30-50% of the total area. We believe that this percentage was adequate for representation.

All histology images were captured using an Olympus Camera DP12 (Japan) integrated with an Olympus BX51 microscope (Japan). The fascicles and remnant nerve fiber components were counted, and endoneurium pore diameters were measured semi-automatically using Fiji, an open-source software program (version 1.54p).

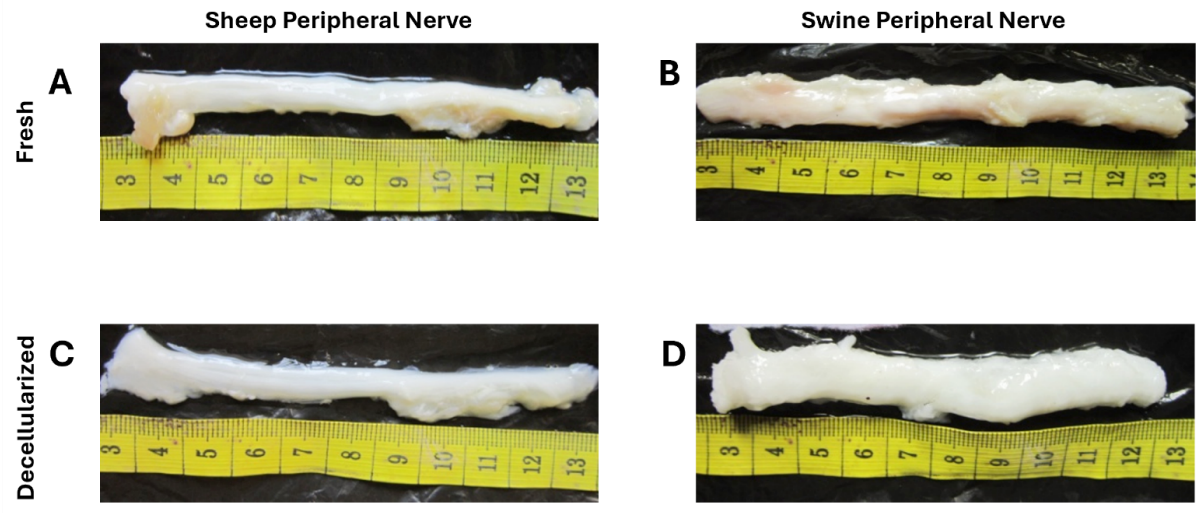


Figure 1. Color of fresh and decellularized nerves

Sheep sciatic nerve: A) Fresh, C) Decellularized; Swine sciatic nerve: B) Fresh, D) Decellularized

Pore diameters were measured after calibrating the scale using the provided scale ba. The distribution of endoneurium pores by diameter was calculated by dividing the number of pores in each diameter category (<3 µm, 3–12 µm, and >12 µm), based on the classification by Oh (2001), by the total number of endoneurium pores measured in one neural fascicle.

Mechanical properties characterization

Distal nerve segments, each 7 cm long, from each group were tested for tensile strength using a universal testing machine (Zwick Z0.5, Germany). For testing, a 3 cm portion of each nerve segment nerves was used, with 2 cm at each end secured in the grips. The samples were kept moist by immersion in PBS during testing. This method was adapted and modified from Borschel et al. (2003). The tensile-strength measurements included maximum force (F) and elongation (%). From these data, the ultimate tensile stress (σmax) and ultimate tensile strain (εmax) were calculated using the Equations 3 and 4 (Choung & Cho, 2008). F_{max} is the maximum force required to fracture the nerve (N); A_0 is the initial cross-sectional area; l_{max} is the maximum nerve length at maximum elongation; l_0 is the initial nerve length.

3. $$\sigma_{max}\,(\mathrm{MPa}) = \frac{F_{max}}{A_0},$$

4. $$\varepsilon_{max} = \frac{l_{max} - l_0}{l_0}$$

Data analysis

Qualitative data, such as macroscopic and histological features, were analyzed descriptively. Quantitative data, including macroscopic, microstructural, and mechanical-strength characteristics, were analyzed statistically using independent-samples t-tests, with a significance level of $P<0.05$, to compare sheep and swine nerves under both fresh and decellularized conditions. SPSS software, version 25 was used for statistical analysis.

Results

Macroscopic characteristics

Fresh peripheral nerves from both sheep and swine appeared reddish due to residual blood. After decellularization, both types of nerves appeared bright white (Figure 1).

Quantitative analysis showed that decellularized sheep peripheral nerves had significantly smaller diameters and cross-sectional areas compared to decellularized swine peripheral nerves. Independent t-test analysis confirmed that these differences were statistically significant ($P<0.05$) (Table 1).

Microstructural histological characteristics

Histological examination revealed more complete decellularization in sheep nerves compared to swine nerves (Figure 2). Fascicles in decellularized sheep nerves appeared clearer and free of residual cellular components,

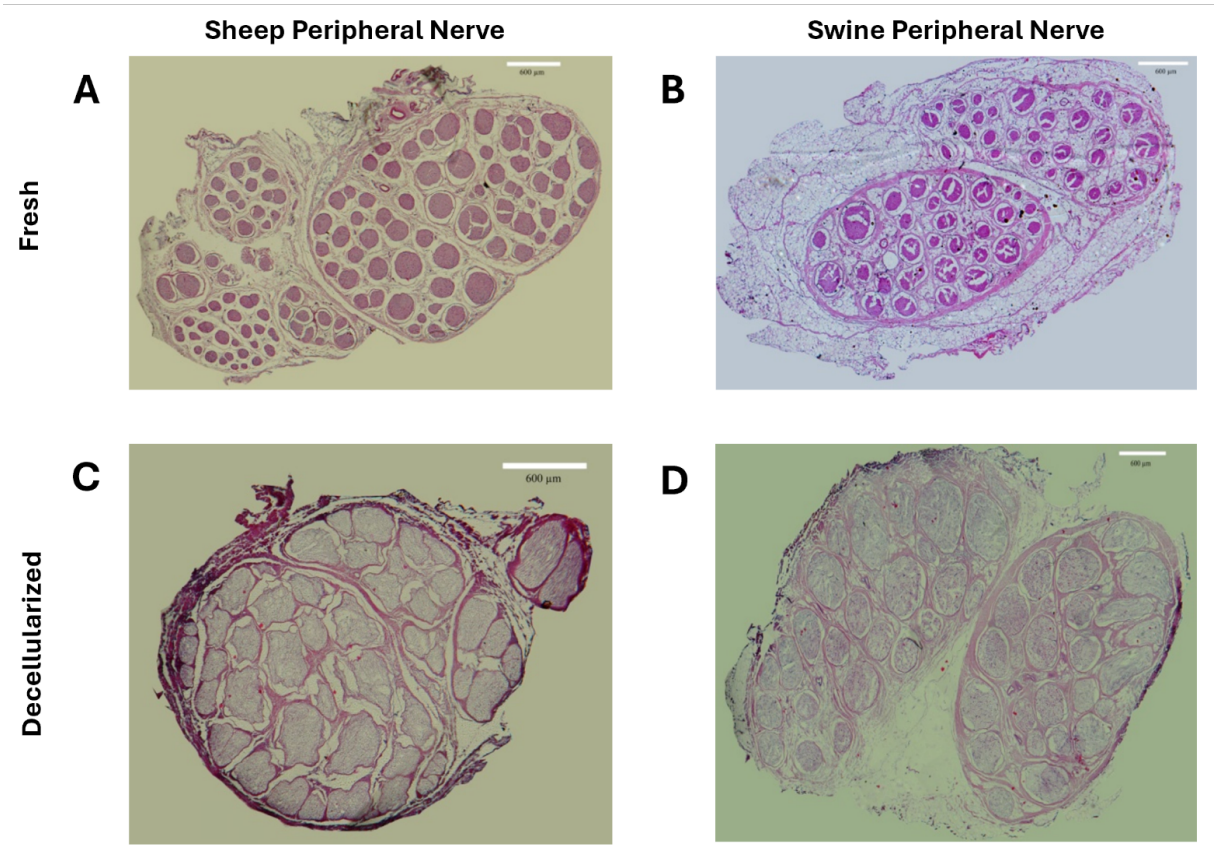


Figure 2. Histological images of peripheral nerves in different groups (H&E stain; scale bar=600 µm)

A) Fresh sheep peripheral nerve with fascicles composed of nerve fibers, B) Fresh swine peripheral nerve with thick adipose tissue in the outer layer and between the fascicles, C) Decellularized sheep peripheral nerve, appearing completely devoid of cells, D) Decellularized swine peripheral nerve, showing the disappearance of adipose tissue (arrow), although the nerve fibers were not completely decellularized

with well-preserved and intact endoneurium pores (Figure 3). In contrast, decellularized swine nerves showed remnants of axons and Schwann cells within endoneurial pores (Figure 3), suggesting incomplete cell removal.

Morphometric analysis showed that the diameter of nerve fascicles in both fresh and decellularized sheep nerves was significantly smaller ($P<0.05$) than that in swine nerves. However, the number of fascicles did not differ significantly between groups ($P>0.05$), suggesting species-related differences in fascicle size but not in fascicle count (Table 1).

Furthermore, decellularized sheep nerve fascicles had significantly fewer residual nerve fiber components than swine nerve fascicles ($P<0.05$, Table 1), again indicating a more efficient decellularization process in sheep. These findings support the qualitative observations of clearer fascicle boundaries and cleaner endoneurial spaces in sheep. In decellularized nerves from both species, endoneurium pore sizes were predominantly within the 3–12 µm and >12 µm ranges (Table 1). Pores smaller than 3 µm were in the minority.

Mechanical properties

Mechanical testing showed distinct differences between fresh and decellularized nerves. Fresh peripheral nerves from both species were mechanically tight, exhibiting high stress and low strain, consistent with the behavior of native collagen-rich biological tissues. After decellularization, sheep nerves became more elastic, exhibiting both high stress and high strain, whereas swine nerves became more compliant, characterized by low stress and high strain (Figure 4).

Statistical analysis using the Mann-Whitney test demonstrated that both decellularized sheep and swine nerves had significantly lower ultimate tensile stress and significantly higher ultimate tensile strain compared to their

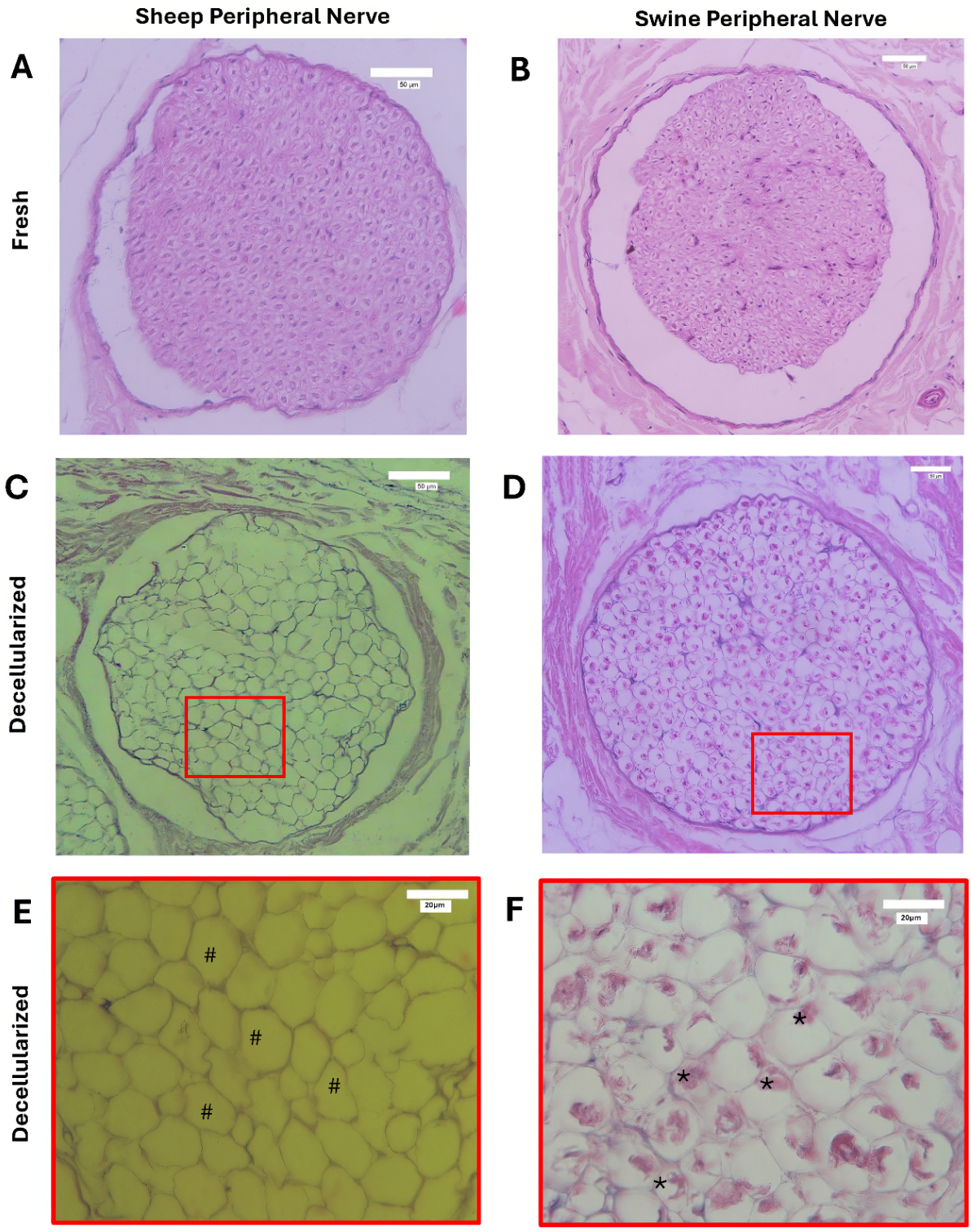


Figure 3. Histological images of peripheral nerve fascicles in the different groups (H&E stain; scale bars: A–D, 50 µm; E–F, 20 µm)

A) Fascicle of a fresh sheep peripheral nerve, B) Fascicle of a fresh swine peripheral nerve, C) Fascicle of a decellularized sheep peripheral nerve, showing intact endoneurial pores and fewer remaining nerve fibers inside the pores; D) Fascicle of a decellularized swine peripheral nerve, showing more remaining nerve fibers, E) Insert of C: the decellularized sheep peripheral nerve has intact endoneurial pores (#) and fewer remaining nerve fiber components inside the pores, F) Insert of D: the decellularized swine peripheral nerve shows more remaining nerve fiber components within the fascicles (*)

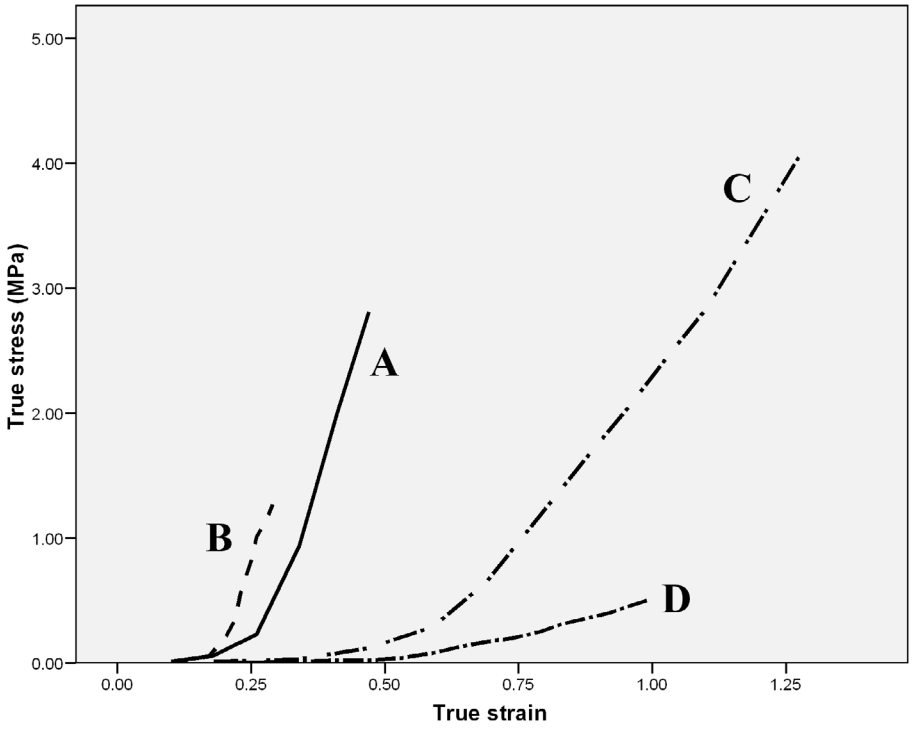


Figure 4. Graph of mechanical properties among groups

A) Fresh sheep nerve, B) Fresh swine nerve, C) Decellularized sheep nerve, D) Decellularized swine nerve

Note: Fresh sheep nerve was more elastic than swine nerve, which was more compliant. Decellularized sheep nerve was more elastic and stronger than decellularized swine nerve, which showed lower stress and higher strain.

fresh counterparts (P<0.05) (Table 1). Notably, decellularized sheep nerves had significantly higher ultimate tensile stress than decellularized swine nerves (P<0.05), suggesting that the absence of extensive adipose tissue in sheep nerves may preserve the structural integrity of the ECM during decellularization. Additionally, significant differences in tensile strain were observed between fresh and decellularized nerves in both species (P<0.05), indicating increased deformability after decellularization.

Discussion

Xenografts are increasingly being explored as scaffold candidates for tissue implants due to their abundance and availability, offering a viable alternative to allografts (Gashtasbi et al., 2020). Peripheral nerves are among the critical tissues requiring regenerative solutions. In this context, sheep and swine have emerged as particularly relevant xenograft donors, as their peripheral nerves share similar histological characteristics with human tissue (Holzer et al., 2022; Pedroza-Montoya et al., 2022). This study investigated the use of explicitly decellularized sheep peripheral nerves as potential substitutes for swine-derived nerve xenografts.

Macroscopic and microstructural findings

Macroscopically, decellularized sheep peripheral nerves exhibited a bright white appearance, consistent with the known characteristics of acellular human peripheral nerves (Yang et al., 2011). At the microstructural level, sheep nerves underwent more complete decellularization than swine nerves, with fewer residual cellular components. This difference is primarily attributed to the thick adipose tissue present in swine nerves, both externally and within the interfascicular spaces. Such tissue likely impeded the penetration of the decellularizing agent, resulting in incomplete cell removal. The lack of lipid in sheep sciatic nerve may be associated with its location in the lumbosacral space, which is protected by large muscles and has fewer lipid deposits.

SDS, an effective decellularization agent, is known for both cell lysis and lipid dissolution (Khosropanah et al., 2024). However, in swine nerves, the abundant adipose tissue likely limited SDS infiltration. Incomplete decellularization is problematic, as remaining cellular elements—particularly those expressing MHC I receptors—can provoke immune rejection after transplantation (Kasravi et al.,

Table 1. Comparison of characteristics between sheep and swine peripheral nerves in fresh and decellularized conditions

Parameter	Parameter	Condition	Sheep	Swine	P
Macroscopic characteristics	Diameter (mm)	Fresh	3.25±0.72	3.76±0.99	0.292
		Decellularized	3.39±0.69	4.6±1.04	0.025*
	Transversal plane area (mm^2)	Fresh	8.62±3.52	11.75±6.15	0.265
		Decellularized	9.34±3.67	17.35±7.5	0.026*
Histological characteristics	Number of remaining nerve fiber components	Decellularized	3.46±2.1	65.11±51.62	0.008*
	Endoneurium pores <3 µm (%)	Decellularized	0.2±0.5	0.47±0.68	0.415
	Endoneurium pores 3–12 µm (%)	Decellularized	50.1±14.81	49.66±14.51	0.957
	Endoneurium pores >12 µm (%)	Decellularized	49.28±14.47	49.73±14.71	0.955
Mechanical characteristics	Ultimate tensile stress (MPa)	Fresh	1.84±1.49	1.17±1.06	0.353
		Decellularized	0.96±1.03	0.15±0.12	0.035*
	Ultimate tensile strain	Fresh	1.07±0.37	0.61±0.3	0.035*
		Decellularized	1.17±0.79	0.99±0.53	0.654

*A significant difference at the P<0.05 level.

2023; Permata et al., 2025). In contrast, the more thorough decellularization observed in sheep nerves indicates a reduced risk of immune response. However, this interpretation is based on histological evidence of reduced cellular remnants rather than direct immunological testing; thus, this result highlights the potency of immunogenicity reduction and the need for confirmation in further studies. We assessed ECM integrity in decellularized samples using only H&E staining, the most common method for visualizing tissue and highlighting endoneurial pores.

The sheep nerves used in this study, sourced from 7-month-old animals, were smaller in diameter than human sciatic, limb, or femoral nerves (Sladjana et al., 2008; Gustafson et al., 2009; Yang et al., 2011). However, nerve size tends to increase with age and body growth, suggesting that older sheep may yield grafts that are more closely matched to human dimensions.

Interestingly, fascicle diameters in decellularized nerves were greater than those in fresh nerves, although the number of fascicles remained similar between sheep and swine. The increase in diameter may be due to water infiltration into the myelin sheath during SDS treatment. Given that the myelin sheath is composed primarily of fat (70–85%) and water (40%), with only 15–30% protein (Poitelon et al., 2020), SDS likely dissolved the lipid content, allowing water to diffuse into the sheath—similar to how adipose tissue affects anesthetic diffusion in human sciatic nerves (Moayeri & Groen, 2009).

Although the decellularized sheep nerves were smaller than adult human nerves—human sciatic nerves typically measure 4.8–6.3 mm in diameter and 18.09–31.16 mm^2 in cross-sectional area (Sladjana et al., 2008), with limb and femoral nerves having similar dimensions (Gustafson et al., 2009; Yang et al., 2011)—larger sheep may provide better anatomical compatibility.

Both decellularized sheep and swine nerves exhibited a higher number of fascicles compared to human sciatic and femoral nerves. While human sciatic nerves contain 27–70 fascicles, and femoral nerves contain 19–47, with diameters of 137.31–259.35 µm and 200–400 µm, respectively (Sladjana et al., 2008; Gustafson et al., 2009). In comparison, our xenogeneic samples displayed even larger fascicle diameters, which were more comparable to those of human femoral nerves than to those of human sciatic nerves.

Additionally, human nerve fibers are classified by diameter: those with a diameter of less than 3 µm are unmyelinated, and those with a diameter of greater than 3 µm are myelinated, with a maximum diameter of 12 µm (Oh, 2001). Our decellularized sheep and swine nerves had a higher proportion of pores greater than 3 µm. Although this differs from human norms, it may be advantageous for grafting applications.

Mechanical properties

The stress-strain behavior of our samples exhibited a J-shaped curve, which is typical of collagen- and neurofilament-rich biological tissues, such as rubber (Pins et al., 1997; Rammensee et al., 2007). Unlike Hookean materials, J-shaped curves suggest an initial compliant phase followed by increasing resistance as the load increases (Santos & Flammang, 2005).

Decellularized sheep nerves were more elastic than their swine counterparts, showing higher stress and strain before failure. In contrast, decellularized swine nerves, although elastic, exhibited brittleness, characterized by low stress and high strain. In general, decellularized nerves of both species had lower ultimate tensile stress and higher ultimate tensile strain than their fresh counterparts. Statistically significant differences in mechanical parameters were found between fresh and decellularized nerves in both species and between sheep and swine nerves.

The disparity in mechanical properties likely stems from tissue composition. Swine nerves contain substantial adipose tissue, which can affect their mechanical integrity and is removed primarily during decellularization, thereby weakening the structure (Marini, 2016). Sheep nerves, in contrast, lack such abundant adipose tissue, which helps preserve their mechanical strength during processing. This finding underscores the significance of ECM components in maintaining structural integrity (Courbot & Elosegui-Artola, 2025).

Collagen—a key ECM component—provides tensile strength due to its triple-helix structure (Wenger et al., 2007; Koopmans et al., 2009). In decellularized nerves, collagen fibers appeared thicker, potentially due to water diffusion facilitated by polar amino acids, such as glutamine and arginine in the collagen sequence (Chow et al., 2018; Qiao et al., 2019). This thickening did not compromise the scaffold's integrity, allowing it to retain its function as a supportive structure for cell attachment.

Compared to human nerves, our decellularized sheep nerves demonstrated comparable or superior mechanical performance. Type I collagen exhibits stress of around 38.44 MPa and strain near 19.03 (Pins et al., 1997), while neurofilament hydrogels show low stress (~0.15×10^{-3} MPa) and high strain (~5.0) (Leterrier et al., 1996). Decellularized sheep nerves exceeded the stress levels of human tibial, peroneal, and even acellular limb nerves, while swine nerves showed lower stress than these tissues. Both xenogeneic nerves displayed higher strain than human sciatic, tibial, and peroneal nerves (Liu, 1948; Sladjana et al., 2008; Gustafson et al., 2009), indicating favorable elasticity for implantation.

Limitations of the study

This study has several limitations that should be acknowledged. Histological sampling was limited to five representative areas per tissue section, which may not fully reflect tissue heterogeneity. Additionally, the use of 2D image-based measurements may introduce bias related to section orientation and tissue anisotropy, particularly when measuring variably shaped structures such as endoneurial pores. Another limitation is that this study used only H&E staining; future studies could use Trichrome Mallory staining to specifically confirm the ECM condition.

We also acknowledge that the different immersion times used for decellularization could contribute to slight biochemical differences, such as differences in matrix protein degradation. Although the methodology provided practical and informative preliminary data, more rigorous quantitative techniques are recommended to strengthen future analyses. Incorporating design-based stereological methods may enhance the accuracy of histological evaluations.

To more accurately confirm the acellularity of peripheral nerve tissue, future studies should include in vitro and in vivo experiments that measure inflammatory cytokines and assess the host immune response. The present study was limited to observing histological and mechanical properties.

Future applications

Decellularized nerve scaffolds contain endoneurial pores—spaces vacated by removed axons and surrounded by ECM. These pores facilitate nutrient diffusion, waste removal, and gas exchange. Scaffolds with pores greater than 50 nm are considered macroporous, a feature that is beneficial for regenerative applications (Gao et al., 2025). Our decellularized sheep nerves meet this criterion and thus provide a strong platform for peripheral nerve repair.

These scaffolds can be enhanced by seeding them with exogenous human neural growth factors or cells. Human mesenchymal stem cells (HMSCs, ~17.9–30.4 µm; based on Ge et al. (2014) and human Schwann cells (HSCs, ~2–5 µm; by Carlsen & Behse, 1980) are ideal candidates. HMSCs can differentiate into tissue-specific

cells, while HSCs play critical roles in axon guidance and remyelination (Sueters et al., 2025). The larger endoneurium pores in our sheep nerves provide ample space to accommodate both cell types, making them ideal for developing functional nerve grafts.

Conclusion

This study demonstrates the potential of decellularized sheep peripheral nerves as superior xenogeneic scaffolds for peripheral nerve repair, particularly when compared to those derived from swine. Decellularized sheep nerves offer a promising, biologically relevant solution for peripheral nerve regeneration in human clinical applications.

Ethical Considerations

Compliance with ethical guidelines

The tissue collection procedure received approval from the Medical Ethics Committee of the Faculty of Medicine, Universitas Brawijaya, Malang, Indonesia (Code: 20/UN10.F08.10/PN/2024).

Funding

This research received no external funding and was supported by personal funds provided by Fajar Shodiq Permata and Rina Susilowati.

Authors' contributions

Conceptualization: Fajar Shodiq Permata, Rini Dharmastiti, and Rina Susilowati; Methodology, software, investigation, resources, and formal analysis: Fajar Shodiq Permata and Muhammad Mirandy Pratama Sirat; Data curation and validation: Rini Dharmastiti and Rina Susilowati; Writing the original draft, visualization, and project administration: Fajar Shodiq Permata; Supervision, review & editing: Rini Dharmastiti and Rina Susilowati; Funding acquisition: Fajar Shodiq Permata and Rina Susilowati; Final approval: All authors.

Conflict of interest

The authors declared no conflict of interest.

References

Azab, E., & Youssef, A. R. (2021). Biocompatibility evaluation of human and porcine acellular dermal matrix on human primary gingival fibroblasts: in vitro comparative study. *European Journal of Dentistry, 15*(3), 563–567. [DOI:10.1055/s-0041-1727551] [PMID]

Borschel, G. H., Kia, K. F., Kuzon, W. M., Jr, & Dennis, R. G. (2003). Mechanical properties of acellular peripheral nerve. *The Journal of Surgical Research, 114*(2), 133–139. [DOI:10.1016/s0022-4804(03)00255-5] [PMID]

Carlsen, F., & Behse, F. (1980). Three dimensional analysis of Schwann cells associated with unmyelinated nerve fibres in human sural nerve. *Journal of Anatomy, 130*(Pt 3), 545–557. [PMID]

Choung, J. M., & Cho, S. R. (2008). Study on true stress correction from tensile tests. *Journal of Mechanical Science and Technology, 22,* 1039-1051. [DOI:10.1007/s12206-008-0302-3]

Chow, W. Y., Forman, C. J., Bihan, D., Puszkarska, A. M., Rajan, R., & Reid, D. G., et al. (2018). Proline provides site-specific flexibility for in vivo collagen. *Scientific Reports, 8*(1), 13809. [DOI:10.1038/s41598-018-31937-x] [PMID]

Contreras, E., Traserra, S., Bolívar, S., Forés, J., Jose-Cunilleras, E., & García, F., et al. (2022). Repair of long nerve defects with a new decellularized nerve graft in rats and in sheep. *Cells, 11*(24), 4074. [DOI:10.3390/cells11244074] [PMID]

Cooper, D. K. C., Wang, L., Kinoshita, K., Habibabady, Z., Rosales, I., & Kobayashi, T., et al. (2023). Immunobiological barriers to pig organ xenotransplantation. *European Journal of Transplantation, 1*(3), 167–181. [Link]

Courbot, O., & Elosegui-Artola, A. (2025). The role of extracellular matrix viscoelasticity in development and disease. *NPJ Biological Physics and Mechanics, 2*(1), 10. [DOI:10.1038/s44341-025-00014-6] [PMID]

Crapo, P. M., Gilbert, T. W., & Badylak, S. F. (2011). An overview of tissue and whole organ decellularization processes. *Biomaterials, 32*(12), 3233–3243. [DOI:10.1016/j.biomaterials.2011.01.057] [PMID]

Deumens, R., Bozkurt, A., Meek, M. F., Marcus, M. A., Joosten, E. A., & Weis, J., et al. (2010). Repairing injured peripheral nerves: bridging the gap. *Progress in Neurobiology, 92*(3), 245–276. [DOI:10.1016/j.pneurobio.2010.10.002] [PMID]

Firdaus, F., Atmoko, B. A., Adinata, Y., Panjaitan, T. S., Krishna, N. H., & Widiyawati, R., et al. (2025). The meta-analysis of sheep body weight prediction with body measurement, breed and sex categories for practical livestock management purposes. *Veterinary Integrative Sciences, 23*(3), 1–10. [DOI:10.12982/VIS.2025.075]

Gabriel, A., Maxwell, G. P., O'Rorke, E., & Harper, J. R. (2024). Performance of human and porcine derived acellular dermal matrices in prepectoral breast reconstruction: a long-term clinical and histologic evaluation. *Aesthetic Surgery Journal, 45*(1), 56–62. [DOI:10.1093/asj/sjae175] [PMID]

Gao, D., Shipman, W. D., Sun, Y., Glahn, J. Z., Beraki, L., & Hsia, H. C. (2025). Macroporous scaffolds based on biomass polymers and their applications in wound healing. *Journal of Bioresources and Bioproducts, 10*(1), 14–31. [DOI:10.1016/j.jobab.2024.12.001]

Gashtasbi, F., Hasannia, S., Hasannia, S., Mahdi Dehghan, M., Sarkarat, F., & Shali, A. (2020). Comparative study of impact of animal source on physical, structural, and biological properties of bone xenograft. *Xenotransplantation, 27*(6), e12628. [DOI:10.1111/xen.12628] [PMID]

Ge, J., Guo, L., Wang, S., Zhang, Y., Cai, T., & Zhao, R. C., et al. (2014). The size of mesenchymal stem cells is a significant cause of vascular obstructions and stroke. *Stem Cell Reviews and Reports, 10*(2), 295–303. [DOI:10.1007/s12015-013-9492-x] [PMID]

Green, M. R., & Sambrook, J. (2012). *Molecular Cloning: A Laboratory Manual*. New York: Cold Spring Harbor Laboratory Press. [Link]

Gu, X., Ding, F., Yang, Y., & Liu, J. (2011). Construction of tissue engineered nerve grafts and their application in peripheral nerve regeneration. *Progress in Neurobiology, 93*(2), 204–230. [DOI:10.1016/j.pneurobio.2010.11.002] [PMID]

Gustafson, K. J., Pinault, G. C., Neville, J. J., Syed, I., Davis, J. A., & Jean-Claude, J., et al. (2009). Fascicular anatomy of human femoral nerve: implications for neural prostheses using nerve cuff electrodes. *Journal of Rehabilitation Research and Development, 46*(7), 973–984. [DOI:10.1682/jrrd.2008.08.0097] [PMID]

Holzer, P., Chang, E. J., Lu, D., Adkins, J., Rogers, K., & Man, A., et al. (2022). 90 Efficacy of porcine skin xenotransplants indistinguishable from allograft in first-in-human clinical evaluation. *Journal of Burn Care & Research: Official Publication of the American Burn Association, 43*(Suppl 1), S60–S61. [DOI:10.1093/jbcr/irac012.093] [PMCID]

Hussain, G., Wang, J., Rasul, A., Anwar, H., Qasim, M., & Zafar, S., et al. (2020). Current status of therapeutic approaches against peripheral nerve injuries: a detailed story from injury to recovery. *International Journal of Biological Sciences, 16*(1), 116–134. [DOI:10.7150/ijbs.35653] [PMID]

Jahnke, S., & Bedi, K. S. (2007). Undernutrition during early life increases the level of apoptosis in the dentate gyrus but not in the CA2+CA3 region of the hippocampal formation. *Brain Research, 1143*, 60–69. [DOI:10.1016/j.brainres.2007.01.109] [PMID]

Kasravi, M., Ahmadi, A., Babajani, A., Mazloomnejad, R., Hatamnejad, M. R., & Shariatzadeh, S., et al. (2023). Immunogenicity of decellularized extracellular matrix scaffolds: a bottleneck in tissue engineering and regenerative medicine. *Biomaterials Research, 27*(1), 10. [DOI:10.1186/s40824-023-00348-z] [PMID]

Khosropanah, M. H., Torabinavid, P., Azimzadeh, A., Tanourlouee, S. B., & Kajbafzadeh, A. M. (2024). Efficient decellularization of human fetal kidneys through optimized SDS exposure. *Scientific Reports, 14*(1), 21545. [DOI:10.1038/s41598-024-71973-4] [PMID]

Koopmans, G., Hasse, B., & Sinis, N. (2009). Chapter 19: the role of collagen in peripheral nerve repair. *International Review of Neurobiology, 87*, 363–379. [DOI:10.1016/s0074-7742(09)87019-0] [PMID]

Leterrier, J. F., Käs, J., Hartwig, J., Vegners, R., & Janmey, P. A. (1996). Mechanical effects of neurofilament cross-bridges. Modulation by phosphorylation, lipids, and interactions with F-actin. *The Journal of Biological Chemistry, 271*(26), 15687–15694. [DOI:10.1074/jbc.271.26.15687] [PMID]

Li, Y., Zhou, Y., Qiao, W., Shi, J., Qiu, X., & Dong, N. (2023). Application of decellularized vascular matrix in small-diameter vascular grafts. *Frontiers in Bioengineering and Biotechnology, 10*, 1081233. [DOI:10.3389/fbioe.2022.1081233] [PMID]

Liu, C. T., Benda, C. E., & Lewey, F. H. (1948). Tensile strength of human nerves; an experimental physical and histologic study. *Archives of Neurology and Psychiatry, 59*(3), 322–336. [DOI:10.1001/archneurpsyc.1948.02300380051004] [PMID]

Marini, F. (2016). Triacylglycerols: characterization and determination. In: B. Caballero, P. M. Finglas & F. Toldrá (Eds.), *Encyclopedia of Food and Health* (pp. 345-350). Academic Press: Elsevier. [DOI:10.1016/B978-0-12-384947-2.00703-0]

Moayeri, N., & Groen, G. J. (2009). Differences in quantitative architecture of sciatic nerve may explain differences in potential vulnerability to nerve injury, onset time, and minimum effective anesthetic volume. *Anesthesiology, 111*(5), 1128–1134. [DOI:10.1097/aln.0b013e3181bbc72a] [PMID]

Oh, S. J. (2001). *Color Atlas of Nerve Biopsy Pathology*. Boca Raton: CRC Press. [DOI:10.1201/9781420039801]

Pedroza-Montoya, F. E., Tamez-Mata, Y. A., Simental-Mendía, M., Soto-Domínguez, A., García-Pérez, M. M., & Said-Fernández, S., et al. (2022). Repair of ovine peripheral nerve injuries with xenogeneic human acellular sciatic nerves prerecellularized with allogeneic Schwann-like cells-an innovative and promising approach. *Regenerative Therapy, 19*, 131–143. [DOI:10.1016/j.reth.2022.01.009] [PMID]

Permata, F. S., Amri, I. A., Nurmaningdyah, A. A., Mahardika, F., Budiarto, S., & Vera, A. K. E., et al. (2026). Antigen removal enhances host tolerance in sheep-derived xenogeneic myocardial scaffold: modulating acute and chronic inflammatory responses in mice. *Regenerative Engineering and Translational Medicine, 12*(1), 236–248. [DOI:10.1007/s40883-025-00417-w]

Permata, F. S., Susilowati, R., Dharmastiti, R., Sirat, M. M. P., & Kartikasari, P. D. (2012). Optimization of tissue decellularization method based on macroscopic and microscopic observation in the sheep peripheral nerves. *Jurnal Sain Veteriner, 30*(2), 61–70. [DOI:10.22146/jsv.2606]

Pins, G. D., Christiansen, D. L., Patel, R., & Silver, F. H. (1997). Self-assembly of collagen fibers. Influence of fibrillar alignment and decorin on mechanical properties. *Biophysical Journal, 73*(4), 2164–2172. [DOI:10.1016/s0006-3495(97)78247-x] [PMID]

Poitelon, Y., Kopec, A. M., & Belin, S. (2020). Myelin fat facts: an overview of lipids and fatty acid metabolism. *Cells, 9*(4), 812. [DOI:10.3390/cells9040812] [PMID]

Qiao, B., Jiménez-Ángeles, F., Nguyen, T. D., & Olvera de la Cruz, M. (2019). Water follows polar and nonpolar protein surface domains. *Proceedings of the National Academy of Sciences of the United States of America, 116*(39), 19274–19281. [DOI:10.1073/pnas.1910225116] [PMID]

Rammensee, S., Janmey, P. A., & Bausch, A. R. (2007). Mechanical and structural properties of in vitro neurofilament hydrogels. *European Biophysics Journal: EBJ, 36*(6), 661–668. [DOI:10.1007/s00249-007-0141-7] [PMID]

Santos, R., & Flammang, P. (2005). Morphometry and mechanical design of tube foot stems in sea urchins: A comparative study. *Journal of Experimental Marine Biology and Ecology, 315*(2), 211-223. [DOI:10.1016/j.jembe.2004.09.016]

Sharmadha, K. L., & Balakrishnan, Y. A. (2024). Comparative analysis of morphological and morphometric features of human, pig, calf, and sheep aortic valves: A cross-sectional study. *International Journal of Anatomy, Radiology and Surgery, 13*(1), AO14–AO17. [DOI:10.7860/IJARS/2024/65881.2968]

Siemens, A. L., Lipsey, R. J., Hedrick, H. B., Williams, F. L., Jr, Yokley, S. W., & Siemens, M. G. (1990). Comparison of market hog characteristics of pigs selected by feeder pig frame size or current USDA feeder pig grade standards. *Journal of Animal Science, 68*(8), 2217–2221. [DOI:10.2527/1990.6882217x] [PMID]

Sladjana, U. Z., Ivan, J. D., & Bratislav, S. D. (2008). Microanatomical structure of the human sciatic nerve. *Surgical and Radiologic Anatomy: SRA, 30*(8), 619–626. [DOI:10.1007/s00276-008-0386-6] [PMID]

Sondell, M., Lundborg, G., & Kanje, M. (1998). Regeneration of the rat sciatic nerve into allografts made acellular through chemical extraction. *Brain Research, 795*(1-2), 44–54. [DOI:10.1016/s0006-8993(98)00251-0] [PMID]

Stang, F., Keilhoff, G., & Fansa, H. (2009). Biocompatibility of Different Nerve Tubes. *Materials, 2*(4), 1480–1507. [DOI:10.3390/ma2041480] [PMCID]

Sueters, J., van Heiningen, R., de Vries, R., Guler, Z., Huirne, J., & Smit, T. (2025). Advances in tissue engineering of peripheral nerve and tissue innervation - a systematic review. *Journal of Tissue Engineering, 16*, 20417314251316918. [DOI:10.1177/20417314251316918] [PMID]

Tuffaha, S. H., Meaike, J. D., & Moran, S. L. (2020). Direct muscle neurotization with long acellular nerve allograft: A case report. *Microsurgery, 40*(2), 258–260. [DOI:10.1002/micr.30498] [PMID]

Wang, X., Chen, L., Ao, Q., Sharma, A., & Sharma, H. S. (2015). Progress in the research and development of nerve conduits. *Translational Neuroscience and Clinics, 1*(2), 97–101. [DOI:10.18679/CN11-6030_R.2015.012]

Wenger, M. P., Bozec, L., Horton, M. A., & Mesquida, P. (2007). Mechanical properties of collagen fibrils. *Biophysical Journal, 93*(4), 1255–1263. [DOI:10.1529/biophysj.106.103192] [PMID]

Wolfe, E. M., Mathis, S. A., Ovadia, S. A., & Panthaki, Z. J. (2023). Comparison of collagen and human amniotic membrane nerve wraps and conduits for peripheral nerve repair in preclinical models: a systematic review of the literature. *Journal of Reconstructive Microsurgery, 39*(4), 245–253. [DOI:10.1055/s-0041-1732432] [PMID]

Yang, L. M., Liu, X. L., Zhu, Q. T., Zhang, Y., Xi, T. F., & Hu, J., et al. (2011). Human peripheral nerve-derived scaffold for tissue-engineered nerve grafts: histology and biocompatibility analysis. *Journal of Biomedical Materials Research. Part B, Applied Biomaterials, 96*(1), 25–33. [DOI:10.1002/jbm.b.31719] [PMID]

Yu, J., Gu, X., & Yi, S. (2016). Ingenuity pathway analysis of gene expression profiles in distal nerve stump following nerve injury: insights into wallerian degeneration. *Frontiers in Cellular Neuroscience, 10*, 274. [DOI:10.3389/fncel.2016.00274]

Zajicek, R., Matouskova, E., Broz, L., Kubok, R., Waldauf, P., & Königova, R. (2011). New biological temporary skin cover XeDerma(®) in the treatment of superficial scald burns in children. *Burns: Journal of The International Society for Burn Injuries, 37*(2), 333–337. [DOI:10.1016/j.burns.2010.07.009] [PMID]

Zhang, Y., Luo, H., Zhang, Z., Lu, Y., Huang, X., & Yang, L., et al. (2010). A nerve graft constructed with xenogeneic acellular nerve matrix and autologous adipose-derived mesenchymal stem cells. *Biomaterials, 31*(20), 5312–5324. [DOI:10.1016/j.biomaterials.2010.03.029] [PMID]